

Article

Optimization Design Method and Experimental Validation of a Solar PVT Cogeneration System Based on Building Energy Demand

Chao Zhou , Ruobing Liang and Jili Zhang *

Faculty of Infrastructure Engineering, Dalian University of Technology, Dalian 116024, China; dutzhouchao@mail.dlut.edu.cn (C.Z.); liangrb@dlut.edu.cn (R.L.)

* Correspondence: zjldlut@dlut.edu.cn; Tel.: +86-411-84706203

Received: 7 July 2017; Accepted: 24 August 2017; Published: 28 August 2017

Abstract: Photovoltaic-thermal (PVT) technology refers to the integration of a photovoltaic (PV) and a conventional solar thermal collector, representing the deep exploitation and utilization of solar energy. In this paper, we evaluate the performance of a solar PVT cogeneration system based on specific building energy demand using theoretical modeling and experimental study. Through calculation and simulation, the dynamic heating load and electricity load is obtained as the basis of the system design. An analytical expression for the connection of PVT collector array is derived by using basic energy balance equations and thermal models. Based on analytical results, an optimized design method was carried out for the system. In addition, the fuzzy control method of frequency conversion circulating water pumps and pipeline switching by electromagnetic valves is introduced in this paper to maintain the system at an optimal working point. Meanwhile, an experimental setup is established, which includes 36 PVT collectors with every 6 PVT collectors connected in series. The thermal energy generation, thermal efficiency, power generation and photovoltaic efficiency have been given in this paper. The results demonstrate that the demonstration solar PVT cogeneration system can meet the building energy demand in the daytime in the heating season.

Keywords: PVT; building energy demand; theoretical analysis; fuzzy control method; experimental study

1. Introduction

Hybrid photovoltaic-thermal collectors are devices for the conversion of solar radiation into electrical and thermal energy simultaneously. Photovoltaic-thermal (PVT) collectors consist of a thin plate made of highly conductive material, on top of which the PV modules are inserted by lamination. Solar radiation is collected and partially converted into electricity. Meanwhile, the circulation of working fluid through the absorber plate plays an important role in removing the excess heat from the PV modules, and then reduces their temperature and potentially improves their photovoltaic efficiency. Low-grade heat can be made available for appropriate uses simultaneously. Therefore, PVT technology, as a deep exploitation and utilization of solar energy, is showing an increasing trend nowadays.

The concept of solar PVT cogeneration systems was first proposed in the late 1970s by Florschuetz [1]. Buker and Riffat gave a clear insight into PVT concept and investigated the future potential of building integrated photovoltaic-thermal collectors [2]. Since then, a large amount of theoretical research has been carried out by a large number of researchers considering water as the working fluid [3–5]. A detailed physical model of a hybrid photovoltaic-thermal system and algorithms for making quantitative predictions regarding the performance of the system was proposed and validated by numerical examples [3]. Along with theoretical research, experimental studies have also been carried out to test the performance of the system [6–9]. An aluminum-alloy flat-box type PVT collector was constructed for domestic water heating purposes which could achieve a high

final hot water temperature after a one-day exposure, and the equipment is capable of extending the PV application potential in the domestic sector [6,7]. Tiwari et al. built up the thermal modeling of a combined system of a PVT solar water heater partially covered with a PV module, and the experimental validation was carried out simultaneously, showing better performance compared with the earlier reported results [9]. A novel building-integrated PVT roof collector, which was an integration of unique polyethylene heat exchanger loop underneath PV modules, was developed and was also combined with a liquid desiccant enhanced dew point cooler by [10,11]. Through the detailed thermal model establishment and experimental research, the results indicated an excellent overall performance and good technical economy of the system. The solar PVT system design method has also drawn the interest of the researchers in recent years. Most of the researchers focused on the theoretical and simulation method based on the performance of PVT collectors and specific building demand when carrying out system design [12–16]. A water-based PVT system was established for an office building in Tse and Chow's study, and performance evaluation and economic analysis of the system were carried out, which reflected the desirable potential of incorporating of PVT technologies in real buildings [13].

The connection of the collector array is an important aspect of system design, which can affect the thermal and electrical efficiency significantly. Plenty of researchers have carried out theoretical, simulation, and experimental studies in this field [17–23]. Rodney et al. built up the mathematical model of collectors connected in series and analyzed the outlet water temperature, thermal energy generation and thermal efficiency [17]. Tiwari et al. carried out a theoretical and experimental study on the PVT water collectors connected in series. Analytical expression and performance evaluation of partially-covered PVT water collectors connected in series was undertaken in this research [18–21]. As for the field of system control method, Sonveer et al. proposed optimized parameters of hybrid dual channel semitransparent photovoltaic thermal module using a fuzzified genetic algorithm [24]. Zhang et al. introduced the fuzzy control method into an air-conditioning system specifically in a low-temperature hot-water radiator system and variable air volume (VAV) terminals, the results of which can be extended to a frequency conversion circulating water pump [25,26]. Other variable speed water pump proper control methods have also been researched [27].

In this study, an optimization design method is carried out for solar PVT cogeneration system based on building energy demand. An academic building is selected as the target building. According to the dynamic heating load and electricity load of the building in the heating season, the solar PVT cogeneration system design is carried out based on the principle of "electricity determines heat". A thermal model of PVT collector is built simultaneously to optimize the connection of the PVT collector array. In addition, the fuzzy control method of frequency conversion circulating water pumps and the pipeline switching control method with electromagnetic valves are introduced in this study to perform system control and energy-saving operation. Along with mathematical analysis, the experimental method has also been validated for the solar PVT cogeneration system. A demonstration of an experimental system is established in Dalian. Through test result analysis and performance evaluation, the conclusion is made that the solar PVT cogeneration system can meet the building's energy demands, implying huge application prospects and promotion value.

2. PVT Collector Description

A structural design scheme of the above-mentioned PVT prototype is shown in Figure 1. The collector measures $L = 2000$ mm in length and $W = 1000$ mm in width, which represents an overall collector surface area $A_c = 2$ m², and is composed of 8 parallel pipes. However, the surface of the thermal absorber is covered by 50 single-crystalline silicon solar cells measuring 156×156 mm connecting in a series, which are applied through a thin adhesive layer called ethylene-vinyl acetate (EVA). In order to enhance the temperature of the thermal absorber, the surface of the thermal absorber is not entirely covered by PV modules. The packing factor, which means the ratio of the surface of the PV modules to the thermal absorber surface, is 0.67 in this research. Then, the glass cover with

a thickness 3 mm is applied to limit the heat losses to the environment and there is an air gap with a thickness 1 mm between the glass cover and the PV modules. The parallel pipes are pressed under the thermal absorber, and then there is a 50-mm-thick insulation layer, which is made of expanded polystyrene (EPS). Table 1 shows the theoretical values of the thermal resistance and heat capacitance of the materials in the PVT collector.

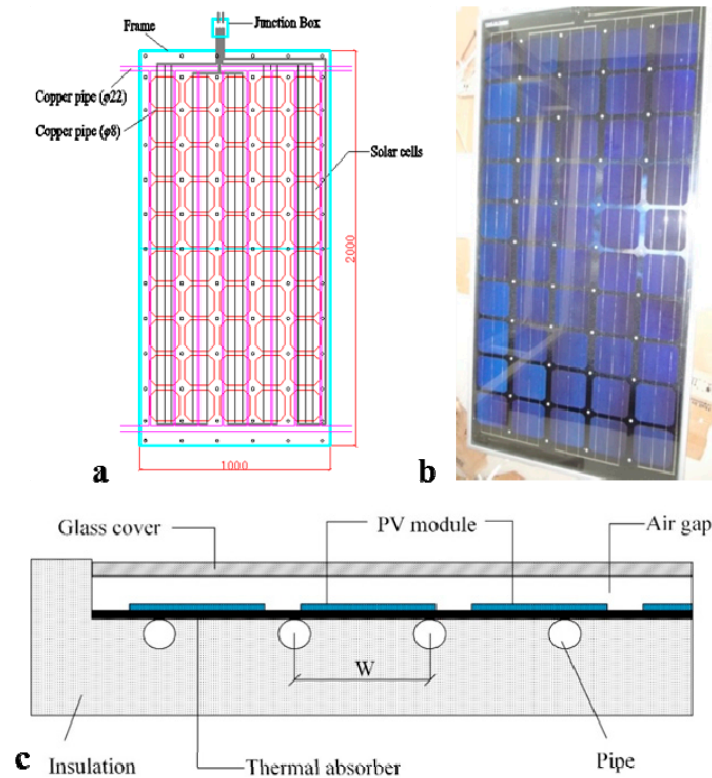


Figure 1. Proposed photovoltaic-thermal (PVT) prototype. (a) Structural schematic; (b) Actual photo; (c) Section view.

Table 1. Material physical properties of the proposed PVT collector.

Material	Thickness (mm)	Density (kg/m ³)	Thermal Conductivity (W/m·K)	R Value (m ² ·K/W)	Heat Capacity (J/kg·K)	Heat Capacitance (J/m ² ·K)
Glass	3.2	3000	1.0	3.2×10^{-3}	500	4800
PV	0.22	2330	148	1.5×10^{-6}	677	355
EVA	0.5	960	0.35	1.4×10^{-3}	2090	1003
Absorber	2	7280	64	0.3×10^{-4}	385	5605
EPS	50	80	0.04	1.2	1120	4480

The section view of the PVT prototype is shown in Figure 1c. The hydraulic connections for the main pipe of the fluid inlet and outlet are placed on a different side of the PVT collector and the outside diameter of the main pipe measures 10 mm. The working fluid runs through a series of parallel pipes made of copper tubes with an outside diameter measuring 8 mm. The eight parallel paths are available for the circulation of the working fluid and the length of the paths is about 2000 mm.

By calculation and testing, the performance parameters including open circuit voltage (U_{oc}), short circuit current (I_{sc}), maximum electrical power (P_{max}), and maximum thermal power (P_{tmax}) for a single PVT collector were obtained and are shown in Table 2.

Table 2. Performance parameters for a single PVT collector. Uoc: open circuit voltage; Isc: short circuit current; P_{tmax}: maximum thermal power; P_{emax}: maximum electrical power.

Parameters (Unit)	Uoc (V)	Isc (A)	P _{emax} (W)	P _{tmax} (W)
Value	33.2	6.1	195	300

3. Building Energy Demand and Solar PVT Cogeneration System Design

3.1. Target Building Overview and Energy Load Calculation

In this study, the Central Air-conditioning Intelligent Control Laboratory (CAIC-Lab) is selected as the target building, which is located at the Institute of Building Energy, Dalian University of Technology, China (coordinates 38.9° N, 121.44° E). It is a single-story building reserved for academics, with an area of 150 m², and a height of 4 m. The building information model (BIM) of the building is built with Revit software, as shown in Figure 2.

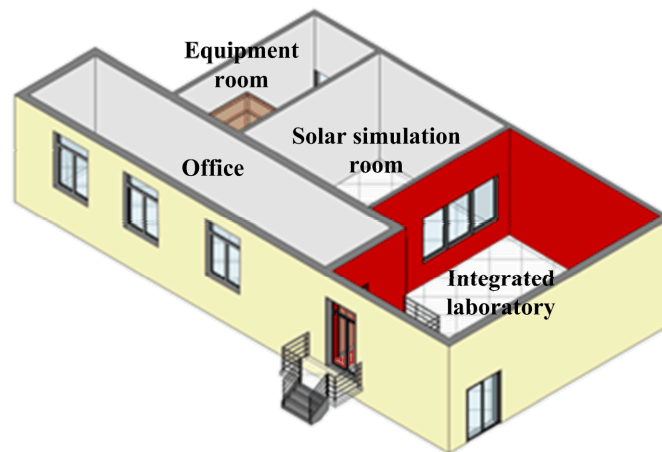


Figure 2. BIM model of the target building.

According to the relevant provisions [28,29], the indoor and outdoor calculation parameters of urban public buildings in winter are as follows: outdoor calculation temperature is -9.8 °C; interior set temperature is 18 °C; the heating season is from November 5 to April 5; and the heating period in one day is from 7:00 a.m. to 18:00 p.m.

3.1.1. Statistical Calculation of Building Electricity Load

The target building is mainly used to test the performance of the central air conditioning intelligent control system for public buildings. Therefore, the annual electricity load mainly comes from air conditioning system equipment and indoor conventional electrical system. Hence, the electricity load can be divided into three categories, namely, wind systems, water systems and conventional electrical systems.

Through statistical calculation, the two-phase power supply load is 7.097 kW and the three-phase power supply load is 13.760 kW. The three-phase power supply load mainly comes from the water system, including the air-cooled heat pump, water-cooled heat pump and circulating water pumps, which are specifically used for air conditioning in summer. In the heating season, this equipment is not in working condition, so the conventional electricity system is the main source of load in winter. Thus, the solar photovoltaic system is designed to work at a 220 V grid-connected mode to meet the building two-phase power load. In this study, taking into account of the simultaneous factor, the designed electricity load of the building is 6 kW. Through statistics calculations according to historical experience, the two-phase electricity load is 30 kWh/day on average.

3.1.2. Calculation of the Building Heating Load

According to the location and envelope structure of the building, the cold air permeation method is used in this study to calculate the heating load in winter, which consists of two parts, building envelope heat consumption and cold air penetration heat consumption.

The building envelope heat consumption can be calculated according to Equation (1) [28]:

$$Q_j = bKAe(T_{a,c} - T_{o,m}) \varepsilon_1 \varepsilon_2 \varepsilon_3 \quad (1)$$

where Q_j is the heating load caused by heat transfer of the building envelope, W; Ae is the area of the envelope, m^2 ; K is the heat transfer coefficient of the building envelope, $W/(m^2 \cdot ^\circ C)$; $T_{a,c}$ is the outdoor calculation temperature, $^\circ C$; $T_{o,m}$ is the interior set temperature, $^\circ C$; b is the temperature correction coefficient; ε_1 is the towards correction coefficient; ε_2 is the outer door correction coefficient; and ε_3 is the height correction coefficient.

The cold air penetration heat consumption can be calculated according to Equation (2) [28]:

$$Q_i = 0.278Aec_p\rho_{ao}(T_a - T_{o,m}) \quad (2)$$

where Q_i is the cold air penetration heat consumption, W; c_p is the specific heat capacity of air, $kJ/(kg \cdot ^\circ C)$; and ρ_{ao} is the density of air, g/L .

Through calculation, the total heating load of the building in winter is 13,335.49 W, and the unit area heating load is $88.90 W/m^2$. In addition, the Trnsys 16 software platform is used in this study to build the target building model and analysis the dynamic heating load fluctuation. The time-varying curves of the heating load of a typical weather day are shown in Figure 3. The steady state calculations of total heating load have a good consistency with the simulation results at nighttime, but they are much higher than those during the daytime because of the strong solar radiation. In this study, the steady state calculation result is selected as the reference value of building heating load when carrying out the system design, so as to ensure the satisfaction of building heating demand.

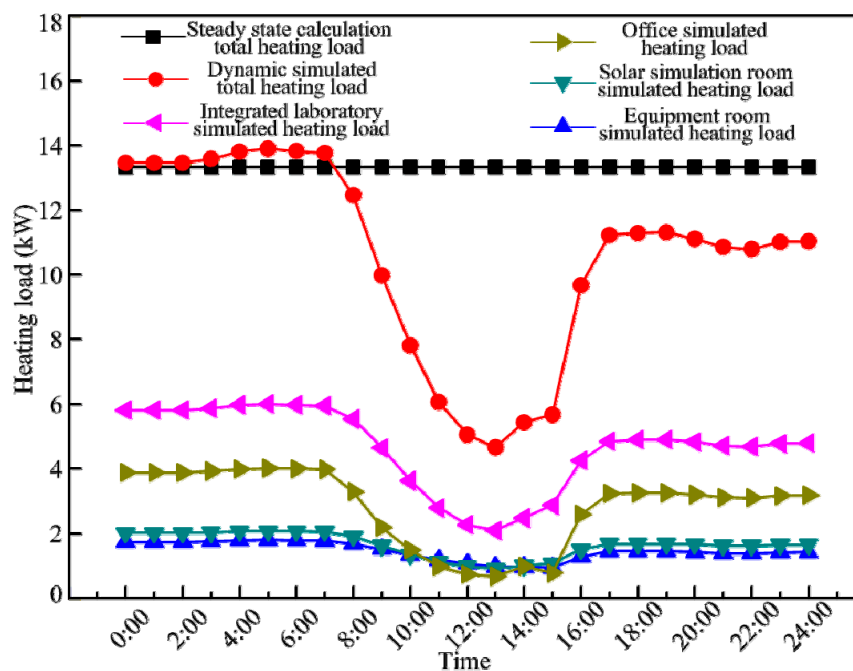


Figure 3. Building steady state calculation heating load and dynamic simulation heating load time-varying curve.

3.2. System Optimization Design

Taking into account the fact that the energy grade of electricity is higher than for thermal energy, and heat energy can be supplemented in various forms whenever it is insufficient, in this study, the “electricity determines heat” principle is used to design the solar PVT cogeneration system. Meanwhile, the calculated building electricity load and dynamic heat load is also the basis for system design to meet the building demand. In this study, the system mathematical model is established and optimized in the selection of series and in the parallel relation of the collector array.

3.2.1. Thermal Modeling

In this study, the same PVT collectors are used, and the system flow rate and heat supply were kept constant. The purpose of system optimization is to determine the number and connection of PVT collectors. Thus, the number of PVT collectors connected in series and in parallel are the two optimization variables to be determined. Several assumptions have been made:

- (1) The heat capacity of PVT collector has been neglected, and the system is in a quasi-steady state;
- (2) The system flow rate is stable, and the Reynolds number for the fluid flowing through the single collector is the same as in the collectors connected in series;
- (3) The energy collected by the system can be effectively used;
- (4) The correction of the total heat loss coefficient and the effective transmittance of module due to the heat loss of the inlet and outlet pipes have been considered;
- (5) The ohmic losses in the solar cell are negligible.

The thermal energy balance for PVT collector is expressed in Equation (3) [30],

$$Q_u = A \cdot F_R [(\tau\alpha)I_t - U_L(T_i - T_a)] \quad (3)$$

The equivalent characteristics when there are M collectors connected in parallel and N connected in series are shown in Equations (4) and (5),

$$F_R(\tau\alpha) = F_{R_1}(\tau\alpha)_1 \cdot \frac{1}{N \cdot K} [1 - (1 - K)^N] \quad (4)$$

$$F_R U_L = F_{R_1} U_{L_1} \cdot \frac{1}{N \cdot K} [1 - (1 - K)^N] \quad (5)$$

where $K = \frac{F_{R_1} U_{L_1}}{\dot{m} C_P} \cdot M \cdot A$.

As above the assumptions state, setting U_d as the heat loss coefficient of the pipe [30], then the corrected collector heat loss coefficient can be expressed as Equations (6) and (7),

$$U'_L = U_L \left[\frac{1 - \frac{U_d \cdot A_i}{\dot{m} C_P} + U_d \frac{A_i + A_0}{A \cdot F_R \cdot U_L}}{1 + \frac{U_d \cdot A_i}{\dot{m} C_P}} \right] \quad (6)$$

$$(\tau\alpha)' = \frac{\tau\alpha}{1 + \frac{U_d \cdot A_0}{\dot{m} C_P}} \quad (7)$$

From the above reasoning, one can get the thermal energy equation of the PVT collector array which is connected in series and in parallel as shown in Equation (8),

$$Q_u \cdot (M \cdot N) = \frac{\dot{m} C_P}{U'_L} [(\tau\alpha)' I_t - U'_L (T_i - T_a)] \left[1 - \left(1 - \frac{A M F_R U'_L}{\dot{m} C_P} \right)^N \right] = \dot{m} C_P (T_0 - T_i) \quad (8)$$

From Equation (9) the collector outlet water temperature can be obtained:

$$T_0 = T_i + \frac{Q_u}{\dot{m}C_P} = T_i + \frac{1}{U'_L} \left[(\tau\alpha)' I_t - U'_L (T_i - T_a) \right] \left[1 - \left(1 - \frac{AMF_R U'_L}{\dot{m}C_P} \right)^N \right] \quad (9)$$

Then, the heating efficiency of the system can be calculated as Equation (10):

$$\eta_{th,N} = \frac{Q_u(MN)}{AI_t} = \frac{\dot{m}C_P}{AI_t U'_L} \left[(\tau\alpha)' I_t - U'_L (T_i - T_a) \right] \left[1 - \left(1 - \frac{AMF_R U'_L}{\dot{m}C_P} \right)^N \right] \quad (10)$$

The PV module is a very important part of PVT collector, and the temperature-affected energy balance of PV module can be expressed as Equation (11) [19]:

$$\alpha_c \tau_g \beta I_t W dx = U_{tc,a} (T_c - T_a) W dx + U_{tc,p} (T_c - T_p) W dx + \eta_c \tau_g \beta I_t W dx \quad (11)$$

From the above equation, the temperature of solar cell can be obtained as Equation (12):

$$T_c = \frac{\alpha_c \tau_g \beta I_t - \eta_c \tau_g \beta I_t + U_{tc,a} T_a + U_{tc,p} T_p}{U_{tc,a} + U_{tc,p}} \quad (12)$$

The energy balance of the heat absorber is shown in Equation (13) [19]:

$$\alpha_p (1 - \beta) \tau_g I_t W dx + U_{tc,p} (T_c - T_p) W dx = F' h_{pf} (T_p - T_f) W dx + U_{tp,a} (T_p - T_a) W dx \quad (13)$$

Then, the temperature of absorber plate can be obtained from Equation (14),

$$T_p = \frac{\alpha_p (1 - \beta) \tau_g I_t + \frac{U_{tc,p}}{U_{tc,p} + U_{tc,a}} (\alpha_c \tau_g \beta I_t - \eta_c \tau_g \beta I_t + U_{tc,a} T_a) + F' h_{pf} T_f + U_{tp,a} T_a}{F' h_{pf} + U_{tp,a} + \frac{U_{tc,a} U_{tc,p}}{U_{tc,a} + U_{tc,p}}} \quad (14)$$

The heat transfer mode between water in the tube and absorber is convection, and the energy balance equation can be expressed as Equation (15):

$$\dot{m}C_P \frac{dT_f}{dx} dx = F' h_{pf} (T_p - T_f) W dx \quad (15)$$

The outlet water temperature of the N th PVT collector connected in series can be obtained according to Equation (9):

$$T_{ON} = T_i + \frac{1}{U'_L} \left[(\tau\alpha)' I_t - U'_L (T_i - T_a) \right] \left[1 - \left(1 - \frac{AMF_R U'_L}{\dot{m}C_P} \right)^N \right] \quad (16)$$

Then the temperature-affected photovoltaic power generation efficiency of the N th PVT collector can be calculated according to Equation (17),

$$\eta_{CN} = \eta_C \left[1 - \theta_{PV} (\overline{T_{CN}} - T_{ref}) \right] \quad (17)$$

To get the average temperature of solar cells of the N th PVT collector $\overline{T_{CN}}$, the average temperature of absorber plate $\overline{T_{pN}}$, and average water temperature $\overline{T_{fN}}$ of the N th PVT collector are needed. The average water temperature $\overline{T_{fN}}$ of the N th PVT collector can be expressed as,

$$\overline{T_{fN}} = \frac{T_{ON} - T_{ON-1}}{2} \quad (18)$$

where T_{ON} and T_{ON-1} can be obtained from Equation (16), so that $\overline{T_{fN}}$ can be expressed as:

$$\overline{T_{fN}} = T_i + \frac{1}{2U'_L} [(\tau\alpha)'I_t - U'_L(T_i - T_a)] \left[2 - \left(1 - \frac{AMF_R U'_L}{\dot{m}C_P} \right)^{N-1} - \left(1 - \frac{AMF_R U'_L}{\dot{m}C_P} \right)^N \right] \quad (19)$$

From Equation (14) and (19), the average temperature of absorber plate $\overline{T_{pN}}$ can be obtained:

$$\overline{T_{pN}} = \frac{\alpha_p(1-\beta)\tau_g I_t + \frac{U_{ic,p}}{U_{ic,p}+U_{ic,a}}(\alpha_c\tau_g\beta I_t - \eta_c\tau_g\beta I_t + U_{ic,a}T_a) + U_{ip,a}T_a + F'h_{pf} \left\{ T_i + \frac{1}{2U'_L} [(\tau\alpha)'I_t - U'_L(T_i - T_a)] \left[2 - \left(1 - \frac{AMF_R U'_L}{\dot{m}C_P} \right)^{N-1} - \left(1 - \frac{AMF_R U'_L}{\dot{m}C_P} \right)^N \right] \right\}}{F'h_{pf} + U_{ip,a} + \frac{U_{ic,a}U_{ic,p}}{U_{ic,a}+U_{ic,p}}} \quad (20)$$

Then, from Equation (12) and (20), the average temperature of solar cells of the N th PVT collector $\overline{T_{CN}}$ can be obtained:

$$\overline{T_{CN}} = \frac{\alpha_c\tau_g\beta I_t - \eta_c\tau_g\beta I_t + U_{ic,a}T_a + \frac{U_{ic,p}}{F'h_{pf} + U_{ip,a} + \frac{U_{ic,a}U_{ic,p}}{U_{ic,a}+U_{ic,p}}} \left\{ \alpha_p(1-\beta)\tau_g I_t + \frac{U_{ic,p}}{U_{ic,p}+U_{ic,a}}(\alpha_c\tau_g\beta I_t - \eta_c\tau_g\beta I_t + U_{ic,a}T_a) + U_{ip,a}T_a + F'h_{pf} \left\{ T_i + \frac{1}{2U'_L} [(\tau\alpha)'I_t - U'_L(T_i - T_a)] \left[2 - \left(1 - \frac{AF_R U'_L}{\dot{m}C_P} \right)^{N-1} - \left(1 - \frac{AF_R U'_L}{\dot{m}C_P} \right)^N \right] \right\} \right\}}{U_{ic,a} + U_{ic,p}} \quad (21)$$

Thus, the photovoltaic power efficiency of the N th PVT collector connected in series can be calculated using Equation (22):

$$\eta_{m \cdot N} = \tau_g \cdot \beta \cdot \eta_{CN} \quad (22)$$

Therefore, the total power generation of the system can be obtained:

$$\dot{Q}_{uel,N} = A \cdot I_t \cdot \sum_1^M \eta_{mN} \quad (23)$$

3.2.2. System Optimization Results

According to the system design requirements, under the premise of meeting the building heat and electrical load demand, the goal of the optimized design is to obtain the highest power generation efficiency and the largest total power generation, as well as the smallest cell temperature. The following constraints are established simultaneously:

- (1) The total photovoltaic power generation of the system should be more than or at least equal to the electrical load demand of the building:

$$C(1) = Q_{electricity} - A \cdot I_t \cdot \sum_1^M \eta_{mN} \leq 0 \quad (24)$$

- (2) The total thermal energy generation of the system should be more than or at least equal to the heat load demand of the building:

$$C(2) = Q_{heat} - \sum \frac{\dot{m}C_P}{U'_L} [(\tau\alpha)'I_t - U'_L(T_i - T_a)] \left[1 - \left(1 - \frac{AMF_R U'_L}{\dot{m}C_P} \right)^N \right] \leq 0 \quad (25)$$

- (3) The outlet water temperature should be higher than or at least equal to the heat supply temperature (it is set at 45 °C in this study):

$$C(3) = 45 - T_i - \frac{1}{U'_L} [(\tau\alpha)'I_t - U'_L(T_i - T_a)] \left[1 - \left(1 - \frac{AMF_R U'_L}{\dot{m}C_P} \right)^N \right] \leq 0 \quad (26)$$

- (4) The system is made up of the same kind of PVT collectors connected in series and in parallel, so the number M and N should be bigger than or at least equal to 1, as shown in Equation (27):

$$\begin{aligned} C(4) &= 1 - M \leq 0 \\ C(5) &= 1 - N \leq 0 \end{aligned} \quad (27)$$

Based on the constraints given above, the objective function model is built. As the “electricity determines heat” principle suggests, the objective function can be defined as the smallest PVT collector array connected in series and in parallel which can meet the demand of the electrical power supply firstly. As shown in Equation (28):

$$f = A_1 \cdot M \cdot N. \quad (28)$$

In solving the above nonlinear optimization problem, values of design parameters used in the computations are shown in Table 3.

Table 3. Values of design parameters used in computations.

Parameter	Value	Unit	Parameter	Value	Unit
A_1	2	m ²	$U_{tc,a}$	9.2	W/(m ² ·K)
A_i	10	m ²	$U_{tc,p}$	5.58	W/(m ² ·K)
A_o	10	m ²	α_c	0.9	
F_R	0.6		τ_g	0.95	
τ	0.95		α_p	0.8	
α	0.8		F'	0.968	
U_L	8.35	W/(m ² ·K)	h_{pf}	100	W/(m ² ·K)
c_p	4180	J/(kg·K)	$U_{tp,a}$	4.74	W/(m ² ·K)
U_d	1	W/(m ² ·K)	θ_{pv}	0.5	%/K
β	0.67		T_{ref}	25	°C
W	1	m	η_{ref}	0.18	

Through calculation, 36 PVT collectors are needed to meet the building heating and electricity load, and the optimization results of PVT collector array connection are shown in Table 4. The optimization calculation is carried out under the condition that the solar radiation intensity is 900 W/m², the ambient temperature is 5 °C, and the inlet water temperature is 10 °C. From the results one can get that a different array connection has almost the same outlet water temperature and is near the thermal efficiency of 41%. The more PVT collectors are connected in parallel, the more thermal energy is generated, but the value maintains at an approximately equal level. As for electricity parameters, the array connection of six PVT connected in series and six groups connected in parallel have the highest amount of total power generation with the highest photovoltaic efficiency. Meanwhile, taking into account the limitation of the installation site, the 6 × 6 PVT collector array is selected as the best connection for the solar PVT cogeneration system.

Table 4. Optimization results of PVT collector array connection.

Number of PVT Collectors Connected in Series (N)	Number of PVT Groups Connected in Parallel (M)	Outlet Water Temperature T_o (°C)	Total Thermal Energy Generation Q_u (MJ)	Thermal Efficiency η_{th} (%)	Total Power Generation Q_e (kWh)	Photovoltaic Efficiency η_e (%)
6	6	14.59	387.15	41.45	28.78	10.9
3	12	14.61	386.02	41.37	28.04	10.8
12	3	14.57	382.97	41.04	27.76	10.5
4	9	14.60	384.99	41.26	28.03	10.7
9	4	14.58	383.30	41.08	27.89	10.6
2	18	14.64	387.09	41.59	28.03	10.8
18	2	14.57	382.63	41.00	27.44	10.3
1	36	14.71	387.48	41.61	28.06	10.8
36	1	14.57	382.30	40.97	26.40	10.1

According to the above design method which is based on the demand of target building heat and electrical load, the system design schematic is shown in Figure 4. The system is made up of 36 PVT collectors which consist of six groups connected in parallel, in there are six connected in series. The thermal energy generated by solar PVT cogeneration system is stored in the storage tank with constant frequency circulating pump 1#. There is an auxiliary heating device set in the storage tank to supply thermal energy when the heat gain from the solar system is insufficient. The thermal energy is supplied to the floor radiant heating system using frequency conversion circulating water pump 2#, to meet the dynamic changes of the heat load in the building. In addition, there are four electromagnetic valves (EV) set in the system to perform the mode switching of the solar system direct heat supply pattern and storage tank heat supply pattern.

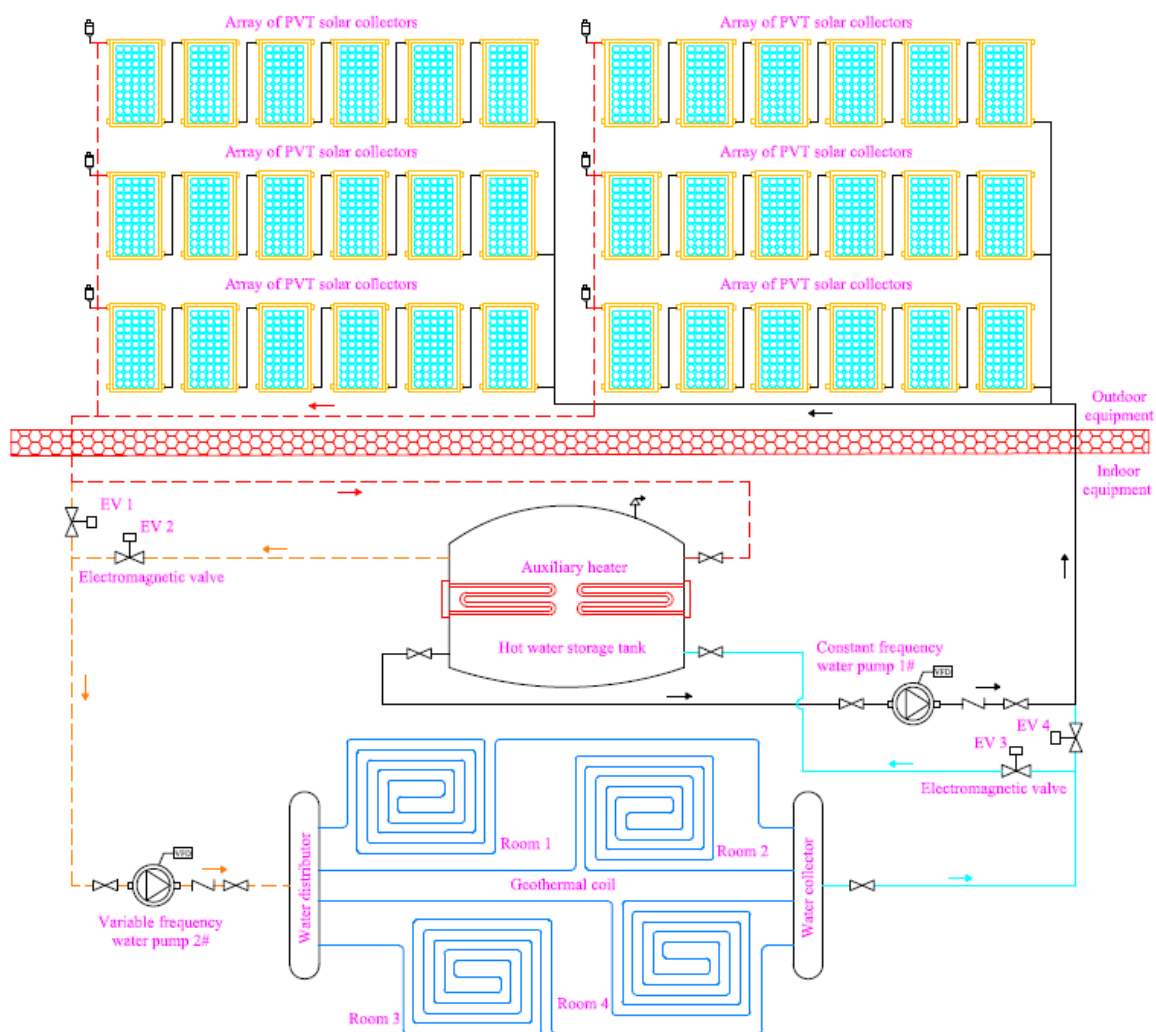


Figure 4. Schematic of proposed solar PVT cogeneration system.

In this study, the grid-connected mode is selected for the solar photovoltaic system. Compared with the off-grid mode, the grid-connected mode has the great advantage of easy installation, flexible equipment configuration, high efficiency, low cost, and easy operation and maintenance. The schematic of the photovoltaic grid-connected system is shown in Figure 5.

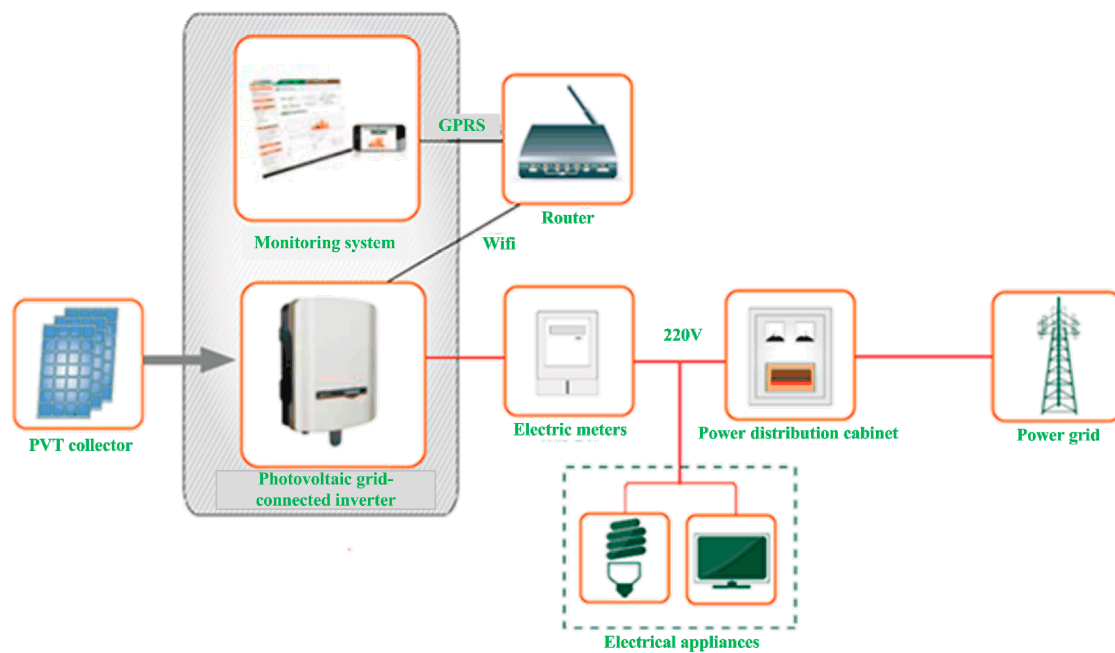


Figure 5. Schematic of photovoltaic grid-connected system.

4. Adjustment and Control Method

Due to the characteristics of strong cyclicity, poor stability and uneven energy density of solar energy resources, the solar PVT cogeneration system will be greatly affected by the solar radiation intensity and the ambient temperature during winter operation. A slight change of meteorological conditions will cause large fluctuations in the amount of electrical and heat generation of the system as well as the heating load and indoor environment. Therefore, it is very important to take a certain strategy to control and adjust the solar PVT cogeneration system according to the dynamic load of the building, and it is also the key to the energy-saving operation.

4.1. Pipeline Switching and Auxiliary Heating Device Control Method

There are four electromagnetic valves in the system and an auxiliary heating device in the storage tank so that the pipeline can be switched according to the building dynamic load and heat generation ability of the system, to ensure the heat supplement. To illustrate the control method, the system is taken schematically as an example, setting the outlet water temperature as T_{FO} , the storage tank water temperature as T_{TANK} , and the geothermal coil water supply temperature as T_{GCI} .

In heating conditions, if $T_{FO} > T_{GCI}$, and the duration is greater than 0.5 h, then open EV1[#] and EV4[#], close EV2[#] and EV3[#], turn on pump 2[#], and turn off pump 1[#]. Now, the hot water generated from the solar system is supplied to the floor radiant heating system directly. If $T_{TANK} < T_{FO} < T_{GCI}$, then open EV2[#] and EV3[#], close EV1[#] and EV4[#], and turn on pump 1[#] and 2[#]. Now the heat gain from solar system stored in the storage tank to heat the water up to 45 °C firstly and then supplied to the building. At this time, if the water supply temperature is lower than 45 °C, the auxiliary heating device is turned on. If $T_{FO} < T_{TANK}$, then open EV2[#] and EV3[#], close EV1[#] and EV4[#], turn on pump 2[#], turn off pump 1[#], and turn on the auxiliary heating device. Now the heating capacity of the solar system is insufficient, and the water in the storage tank is heated to the set point of water supply temperature by the auxiliary heating device, and then supplied to the building.

In non-heating conditions, if $T_{FO} > T_{TANK}$, then open EV2[#] and EV3[#], close EV1[#] and EV4[#], turn on pump 1[#] and turn off pump 2[#]. Now, the heat generated from the solar system is stored in the storage tank and supplied to the building as domestic hot water. If insufficient, the auxiliary heating device is turned on. If $T_{FO} < T_{TANK}$, turn off pump 1[#] and 2[#]. At this time the system is stopped.

The control flow chart of pipeline switching and auxiliary heating device control method is shown in Figure 6.

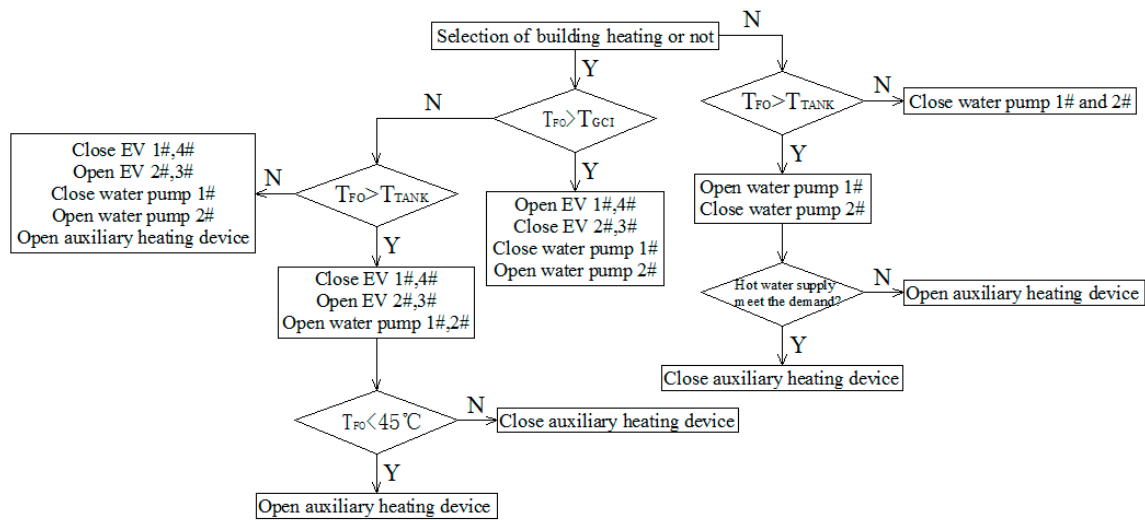


Figure 6. Control flow chart of pipeline switching and auxiliary heating device control method.

4.2. Circulating Water Pump Frequency Conversion Control Method

In order to perform the energy saving and dynamic load-adapted operation of solar PVT cogeneration system, circulating water pump 2[#] runs at frequency conversion mode. When the system runs on heating conditions and in non-direct heating mode, the fuzzy control logic is used in this study to adjust the working frequency of circulating water pump 2[#]. The work principle and control method of fuzzy logic is illustrated as follows:

The room set temperature is assumed as T_{RS} , measured room temperature as T_{RT} , the difference between measured room temperature and room set temperature as eT ($eT = T_{RT} - T_{RS}$), and the variety of room temperature deviation as ecT (it can be defined as the difference between the current and previous room temperature deviation). The control method is based on the “ eT and ecT jointly determined pump frequency stalls” principle as shown in Figure 7.

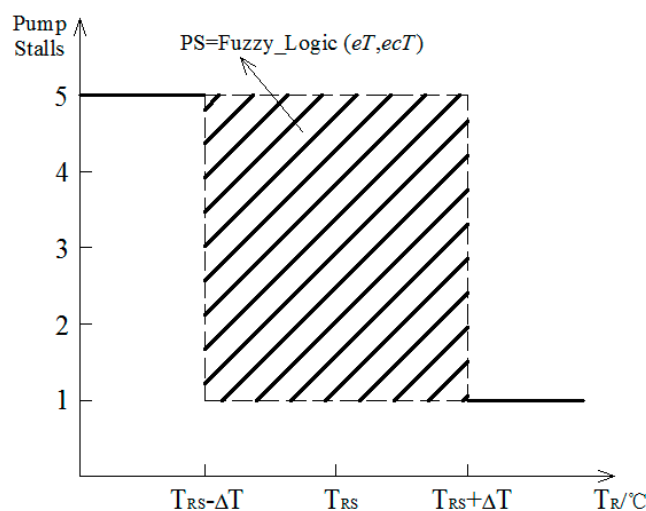


Figure 7. Schematic of variable frequency stall control method for the circulating water pump.

The values of the input variables are defined as the values of the language variables of the fuzzy set. The fuzzy domain of eT and ecT is taken as $[-2, 2]$ and divided into five fuzzy levels, including (NB: negative big, NS: negative small, ZE: zero, PS: positive small, PB: positive big). The triangular subordinate function is selected for the input variables as shown in Figure 8. The fuzzy reasoning values for the output frequency f can be divided into five stalls as: $f = \{1:29.2 \text{ HZ}, 2:36.8 \text{ HZ}, 3:42.2 \text{ HZ}, 4:46.4 \text{ HZ}, 5:50 \text{ HZ}\}$. The functioning-fuzzy-subset inference (FFSI) method is selected as the fuzzy reasoning method. Based on the control objectives to be achieved, the fuzzy control strategy is generated. For example, if ($eT = \text{NB}$ and $ecT = \text{NB}$), then ($f = 5$), if ($eT = \text{PB}$ and $ecT = \text{PB}$), then ($f = 1$) and so on.

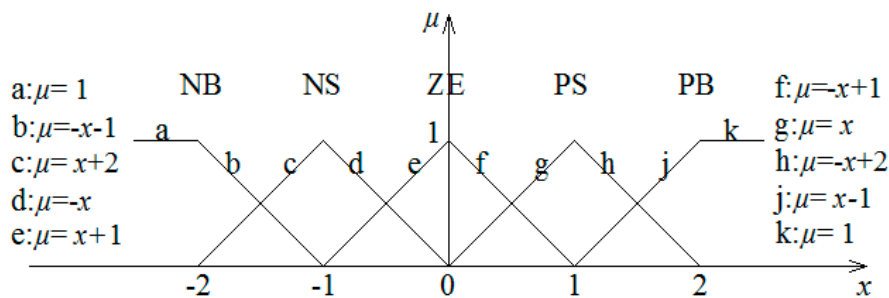


Figure 8. Subordinate function.

Since the input variables eT and ecT have five language variables respectively, the fuzzy control logic consists of 25 control rules. In this study, by setting up experimental platform and fitting method, the fuzzy control rules are obtained as shown in Table 5. For example, when $eT = \text{NS}$ and $ecT = \text{NS}$, it means the current room temperature is lower than the set temperature with NS level, and the current temperature deviation is lower than the previous one with NS level, so it shows a decreasing trend in room temperature. Thus, circulating water pump 2[#] runs at the fourth stall. When $eT = \text{ZE}$ and $ecT = \text{ZE}$, it represents that the current room temperature is equal to the set temperature and the temperature deviation remains constant. Hence, the room temperature is stable, and under this condition circulating water pump 2[#] runs at the third stall.

Table 5. Fuzzy control rules for frequency conversion circulating water pump 2[#].

$eT \backslash ecT$	NB	NS	ZE	PS	PB
NB	5	5	4	3	3
NS	5	4	3	3	2
ZE	4	4	3	2	2
PS	4	3	2	2	1
PB	3	3	2	1	1

The control flow chart of the fuzzy control method for circulating water pump 2[#] is shown in Figure 9. In addition to the control strategy, taking into account the sudden changes in heating load on the impact of room temperature control, there is a specific control strategy according to real-time room temperature changes. If $T_{RT} < (T_{RS} - \Delta T)$ and the duration lasts more than 10 min, circulating water pump 2[#] automatically transferred to fifth stall. If $T_{RT} > (T_{RS} + \Delta T)$ and the duration last more than 10 min, circulating water pump 2[#] automatically transferred to the first stall.

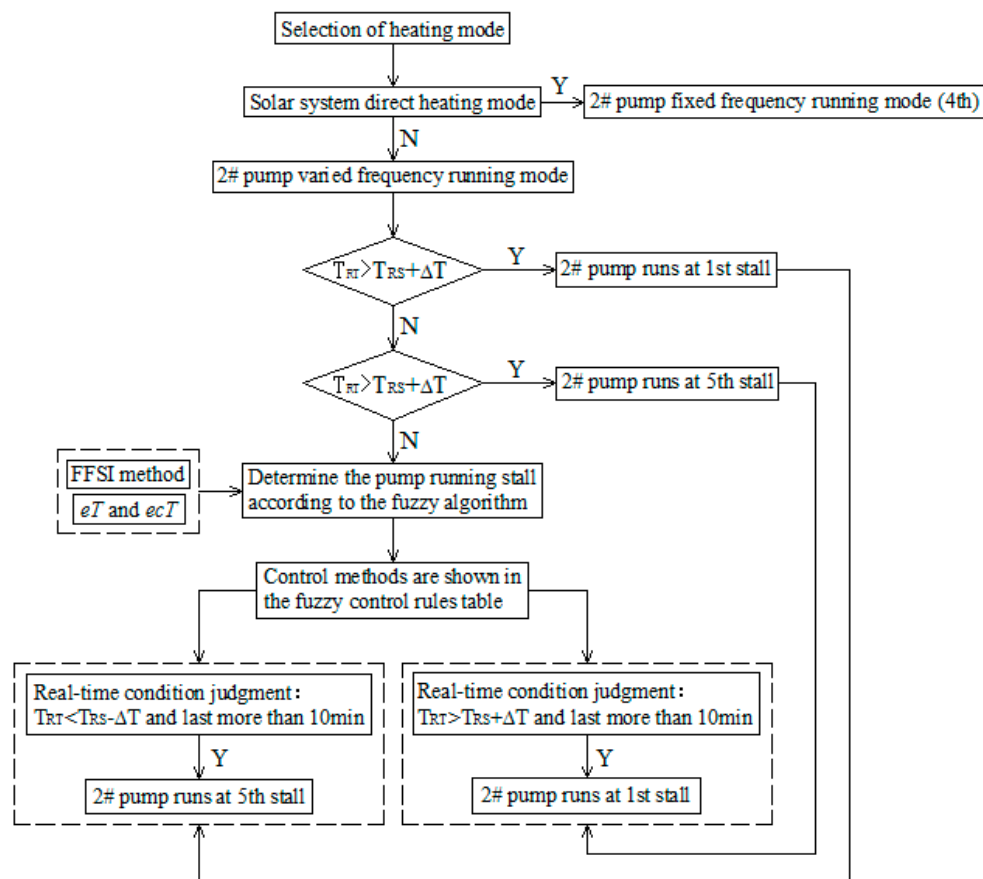


Figure 9. Control flow chart of the fuzzy control method for circulating water pump 2#.

5. Experimental Study and Results Analysis

Based on the above theoretical analysis and system optimization design method, in order to study the performance of solar PVT cogeneration system and the prospect of large-scale engineering applications in northern of China, this study constructed a demonstration of an experimental system with the rated electricity capacity of 7.56 kWp to supply electrical and thermal energy to the target building. Through experiment results, one can analyze the performance and make an economic evaluation of the system.

The experimental setup is constructed near the target building (coordinates N38.9°, E121.44°). The solar PVT cogeneration system consists of 36 PVT collectors with installation angle of 39°, a storage tank with a volume of 2 tons, an auxiliary heating device, constant frequency circulating water with pump 1#, frequency conversion circulating with water pump 2#, 4 electromagnetic valves, and a set of monitoring systems. Two sub-catchments are used to supply hot water to the building floor radiant heating. The schematic of the system after complete construction is as shown in Figure 10.

The monitoring system is mainly composed of five parts. The environment parameters of each room are measured by the temperature and humidity self-recording module. The water temperature measurement uses a self-made Pt100 temperature sensor. The flow rate of water system is measured by the ultrasonic flow meter. The outdoor meteorological parameter test uses PC-4 the meteorological station. Some of the test instruments used in this study are shown in Figure 11.



Figure 10. Schematic of the demonstration experimental system.

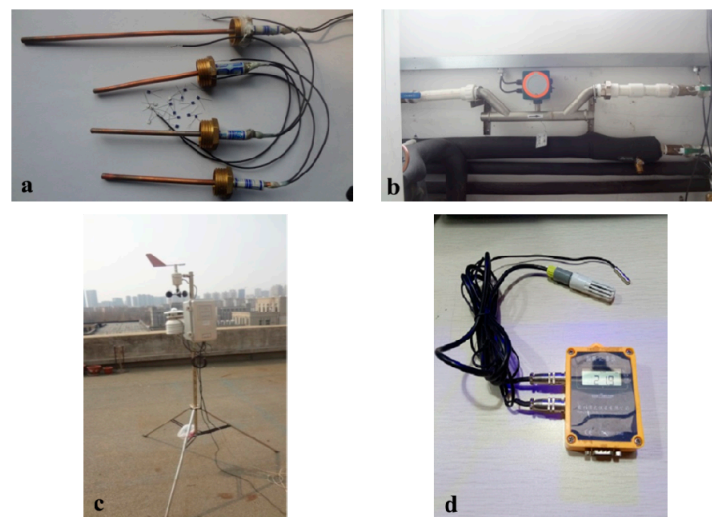


Figure 11. Test instruments: (a) Pt100 temperature sensor; (b) Ultrasonic flow meter; (c) PC-4 meteorological station; (d) Temperature and humidity self-recording module.

An uncertainty analysis of the reduced data is conducted, based on the propagation of error method. Accuracies for various test instruments are given in Table 6. For a moderate flow rate and solar radiation intensity, the uncertainty in heat efficiency was about 6%. Higher uncertainties were found at lower solar radiation intensity.

Table 6. Uncertainties of various test instruments.

Parameters	Uncertainties
Ultrasonic flow meter	$\pm 0.5\%$
Pt100 temperature sensor	± 0.1 K
Solar radiation intensity	$\pm 5\%$
Ambient temperature sensor	± 0.5 °C
Ambient humidity sensor	$\pm 2\%$
Temperature self-recording module	± 0.1 °C
Humidity self-recording module	$\pm 1\%$

The experiment was carried out in winter heating season for one month. The test results of a typical weather day are taken as an example to illustrate the experimental results. The meteorological parameter time-varying curve is shown in Figure 12a. Solar radiation intensity varies in a parabolic form during the day and reaches peak point 900 W/m^2 at 12:00 p.m. From 10:00 a.m. to 1:00 p.m., the value of solar radiation intensity is higher than 800 W/m^2 . The ambient temperature increases in the daytime and varies from $1 \text{ }^\circ\text{C}$ to $6 \text{ }^\circ\text{C}$. Meteorological parameters are the basis of system performance analysis.

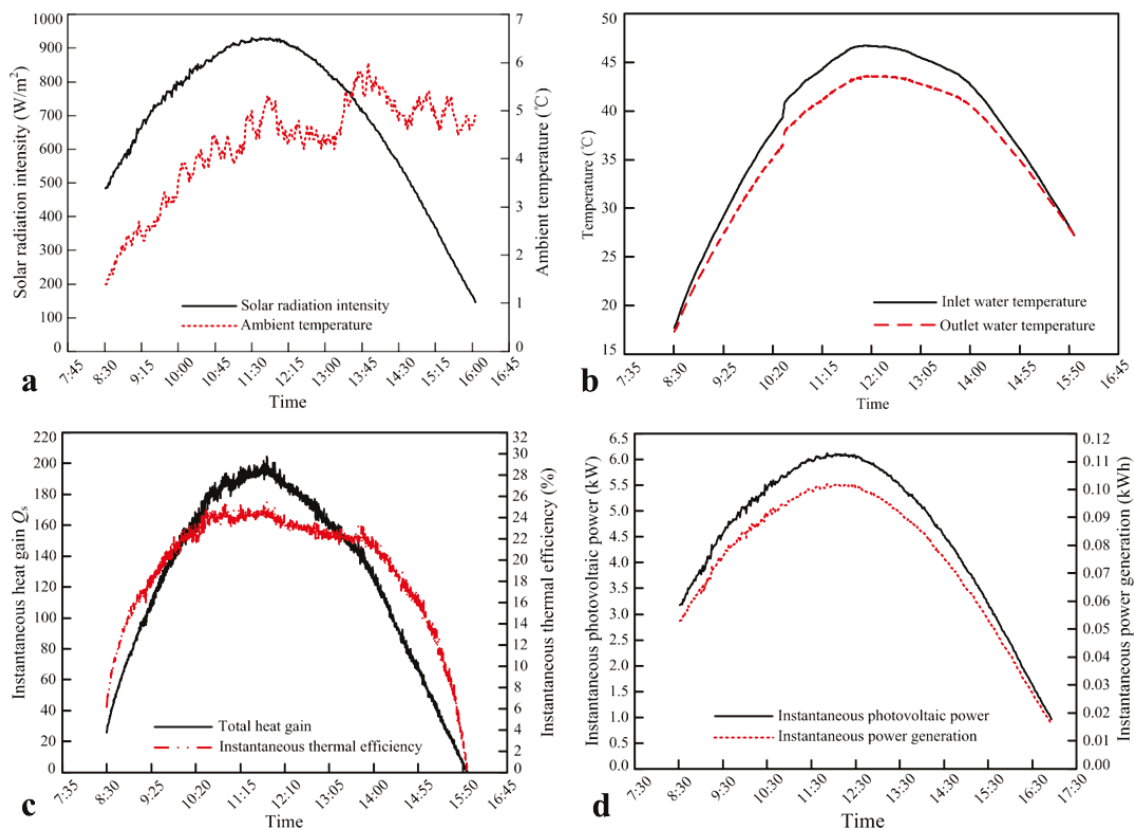


Figure 12. Experiment results: (a) Meteorological parameters time-varying curve; (b) Inlet and outlet water temperature time-varying curve; (c) Amount of thermal energy generation time-varying curve; (d) Amount of photovoltaic power generation time-varying curve.

The inlet and outlet water temperature time-varying curves are shown in Figure 12b. They also vary in a parabolic manner and the temperature difference reaches a peak point of $4.2 \text{ }^\circ\text{C}$ at 12:30 p.m. Compared with solar radiation intensity, there is a half-hour delay in variation. The greater the temperature difference between the inlet and outlet water, the more heat is obtained from the system. Through statistics calculation, the system can reach an average temperature difference of $2.5 \text{ }^\circ\text{C}$ for 4 h per day in heating season. The thermal energy obtained by the system can meet the heating load of the building on average in the daytime.

The amount of thermal energy generation time-varying curve is shown in Figure 12c. The results show that the maximum instantaneous heat gain is 205 kJ and the maximum thermal efficiency is 27%. The total heat gain in the typical day is 320 MJ with the average thermal efficiency of 25%. Because of the existence of packing factor, the thermal efficiency of PVT collector is lower than the traditional flat solar collectors with 100% endothermic area. The amount of photovoltaic power generation can be seen in Figure 12d. From the results one can get that, the instantaneous photovoltaic power varies with the solar radiation intensity and its time-varying curve looks like parabolic. The maximum

photovoltaic power in the daytime is 6.12 kW, and the accumulated power generation in the typical day is 38.37 kWh. Taking into account the existence of various losses, the photovoltaic efficiency is about 10%.

Each measured room temperature and ambient temperature time-varying curve are shown in Figure 13. Because of the location, function and envelope structure of different rooms, the temperature of each room shows different trends in the day. The office is on the south face and there is a glass skylight in the part of the integrated laboratory. The two rooms are used as a workplace for teachers and students. Otherwise, the solar simulation room and equipment room are on the north face and nobody works there usually. Hence, the temperature trend can be explained in that the office temperature remains at 24 °C to 26 °C, and the solar simulation room and equipment room temperature remains at 18 °C to 20 °C. The integrated laboratory room temperature fluctuates more than others because of the solar direct radiation into the room through the glass skylight, and varies between 18 °C and 24 °C.

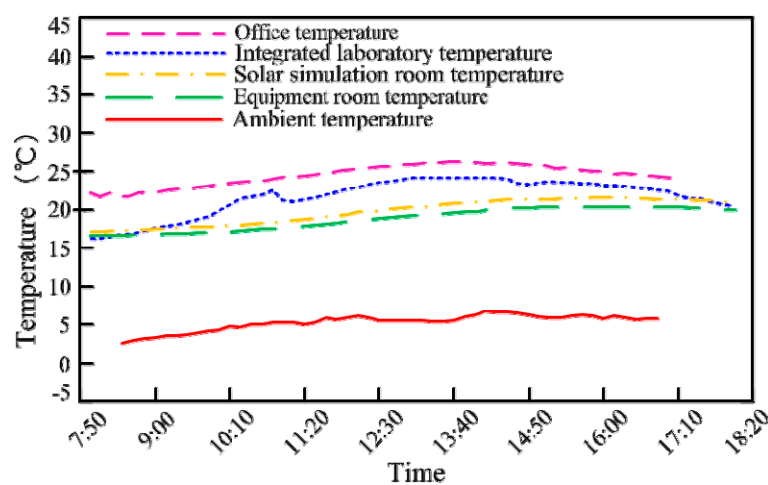


Figure 13. Measured room temperature time-varying curve.

In summary, the performance test results concluded from the one-month heating season experiment are shown in Table 7. On average, the accumulated thermal energy generation in one day is 288 MJ, which can meet the 54.5% of the building heating load demand over the whole day, which can fully meet the heating load in the daytime. The room temperature in the building can reach the set point and maintain it in the daytime. Meanwhile, the accumulated power generation is 32 kWh, which can fully meet the building electricity load demand.

Table 7. Performance test results in heating season.

Parameters	Unit	Values
Accumulated thermal energy generation in one day	MJ	288
Average thermal efficiency	%	23
Average temperature difference between inlet and outlet	°C	3
Average photovoltaic power	kW	6.1
Accumulated power generation	kWh	32
Photovoltaic efficiency	%	10

6. Conclusions

This paper proposes a solar PVT cogeneration system that consists of novel PVT collectors that can generate thermal energy and electric energy simultaneously. The aim of this paper is to carry out optimization design of solar PVT cogeneration system based on the building energy demand and the theoretical analysis of the system thermal model. An academic building located in the Dalian

University of Technology is selected as the target building. The dynamic heating load and electricity load is calculated and simulated through statistics and Trnsys platform, which is the basis of system design. Then, the thermal model of PVT collector and the system connection of collector array is derived by using basic energy balance equations. Several assumptions and constraints are established simultaneously, and then optimization results show that different array connection has almost the same outlet water temperature and near-thermal efficiency. The more PVT collectors are connected in parallel, the more thermal energy generated, but the value is maintained at an approximately equal level. However, the array connection of 6 PVT collectors connected in series and 6 groups connected in parallel shows the highest amount of total power generation with the highest photovoltaic efficiency. Hence, the 6×6 PVT collector array is selected as the best connection for the solar PVT cogeneration system in this paper.

In order to realize the optimum control adjustment and energy-saving operation, this study introduces the fuzzy control method of frequency conversion circulating water pumps and pipeline switching with electromagnetic valves to adapt the fluctuation of the dynamic heating load. The control method is shown in detail in this paper.

In addition, an experimental study is carried out simultaneously. The demonstration experimental system is established near the target building with the rated electricity capacity of 7.56 kWp. The results illustrate that, on average, the accumulated thermal energy and power generation can meet the heating load of the building in the daytime. The average thermal efficiency of the system is 23% with a photovoltaic efficiency of 10%. Meanwhile, the room temperature in the building can reach the set point and maintain it in the daytime. Furthermore, the system always runs at the optimum operating point by using the above-mentioned control method.

Acknowledgments: This study is supported by National Key Research and Development Project of China (Grant No. 2017YFC0704202) and National Natural Science Foundation of China (Grant No. 51676026), supported by Dalian Municipal Science and Technology Plan Project (Grant No. 2015E11SF055, 2015E11SF053) and the Dalian University of Technology under Scientific Research Startup Funding (DUT16RC(4)21).

Author Contributions: Jili Zhang, Ruobing Liang and Chao Zhou conceived and designed the experiments; Chao Zhou performed the experiments; Chao Zhou analyzed the data; Ruobing Liang built the BIM model of the building; Chao Zhou carried out the theoretical analysis of the system; Jili Zhang contributed materials and analysis tools; Chao Zhou wrote the paper; all authors revised and approved the manuscript.

Conflicts of Interest: The authors declare no conflict of interest.

Nomenclature

Q_j	the heating load caused by heat transfer of the building envelope, W
A_e	the area of the envelope, m^2
K	the heat transfer coefficient of the building envelope, $W/(m^2 \cdot ^\circ C)$
$T_{a,c}$	the outdoor calculation temperature, $^\circ C$
$T_{o,m}$	the interior set temperature, $^\circ C$
b	the temperature correction coefficient
ε_1	the towards correction coefficient
ε_2	the outer door correction coefficient
ε_3	the height correction coefficient
Q_i	the cold air penetration heat consumption, W
c_p	the specific heat capacity of air, $kJ/(kg \cdot ^\circ C)$
ρ_{ao}	the density of air, g/L
Q_u	the heat gain of PVT collector, W
A	the area of PVT collector, m^2
A_i	the outer surface area of the inlet water pipe, m^2
A_o	the outer surface area of the outlet water pipe, m^2
F_R	the collector heat transfer factor
τ	the transmittance of the PVT collector glass cover

α	the absorptivity of solar PV module
I_t	solar radiation intensity, W/m^2
U_L	overall heat transfer coefficient of the absorber plate, $W/(m^2 \cdot K)$
T_i	inlet water temperature, $^{\circ}C$
T_o	outlet water temperature, $^{\circ}C$
T_a	ambient temperature, $^{\circ}C$
N	number of PVT collectors connected in series
M	number of PVT collectors connected in parallel
\dot{m}	the rate of flow of water mass, kg/s
C_p	the specific heat of working fluid, $J/(kg \cdot K)$
$\eta_{th,N}$	the heating efficiency of the system
η_{CN}	the temperature affected photovoltaic power generation efficiency of the Nth PVT collector
η_C	the photovoltaic efficiency of the solar cell under standard test conditions
T_{ON}	the outlet water temperature of the Nth PVT collector connected in series, $^{\circ}C$
T_{CN}	the temperature of solar cells of the Nth PVT collector, $^{\circ}C$
T_{fN}	the water temperature of the Nth PVT collector, $^{\circ}C$
T_{pN}	the temperature of absorber plate of the Nth PVT collector, $^{\circ}C$
η_{mN}	the photovoltaic power efficiency of the Nth PVT collector connected in series
$Q_{uel,N}$	the total power generation of the system, W
U_d	overall heat transfer coefficient of the water pipe, $W/(m^2 \cdot K)$
β	the packing factor of PVT collector
L	the length of PVT collector, m
W	the width of PVT collector, m
$U_{tc,a}$	overall heat transfer coefficient from cell to the ambient from top surface, $W/(m^2 \cdot K)$
$U_{tc,p}$	overall heat transfer coefficient from cell to the absorber plate, $W/(m^2 \cdot K)$
$U_{tp,a}$	overall heat transfer coefficient from the absorber plate to the ambient, $W/(m^2 \cdot K)$
T_c	temperature of the solar cell, $^{\circ}C$
T_p	temperature of the absorber plate, $^{\circ}C$
τ_g	the transmittance of the solar PV module glass cover
α_c	the absorptivity of solar cell
α_p	the absorptivity of the absorber plate
F'	the collector efficiency factor
h_{pf}	the heat transfer coefficient from the absorber plate to the water, $W/(m^2 \cdot K)$
θ_{PV}	temperature coefficient of solar PV module, $\%/K$
T_{ref}	temperature of standard test conditions, $25^{\circ}C$ in this study

References

1. Florschuetz, L.W. Extension of the Hottel-Whillier model to the analysis of combined photovoltaic/thermal flat plate collectors. *Sol. Energy* **1979**, *22*, 361–366. [[CrossRef](#)]
2. Buker, M.S.; Riffat, S.B. Building integrated solar thermal collectors—A review. *Renew. Sustain. Energy Rev.* **2015**, *51*, 327–346. [[CrossRef](#)]
3. Bergene, T.; Lovvik, O.M. Model calculation on a flat-plate solar heat collector with integrated solar cells. *Sol. Energy* **1995**, *55*, 453–462. [[CrossRef](#)]
4. Garg, H.P.; Agarwal, R.K. Some aspects of a PV/T collector: Forced circulation flat plate solar water heater with solar cells. *Energy Convers. Manag.* **1995**, *36*, 87–99. [[CrossRef](#)]
5. Chow, T.T. Performance analysis of photovoltaic-thermal collector by explicit dynamic model. *Sol. Energy* **2003**, *75*, 143–152. [[CrossRef](#)]
6. Chow, T.T.; He, W.; Ji, J. Hybrid photovoltaic-thermosiphon water heating system for residential application. *Sol. Energy* **2006**, *80*, 298–306. [[CrossRef](#)]
7. He, W.; Chow, T.T.; Ji, J.; Lu, J.; Chan, L. Hybrid photovoltaic and thermal solar-collector designed for natural circulation of water. *Appl. Energy* **2006**, *83*, 199–210. [[CrossRef](#)]
8. Hocine, H.B.C.; Touafek, K.; Kerrour, F. Theoretical and experimental studies of a new configuration of photovoltaic-thermal collector. *J. Sol. Energy Eng* **2017**, *139*, 021012. [[CrossRef](#)]

9. Dubey, S.; Tiwari, G.N. Thermal modeling of a combined system of photovoltaic thermal (PV/T) solar water heater. *Sol. Energy* **2008**, *82*, 602–612. [[CrossRef](#)]
10. Buker, M.S.; Mempo, B.; Riffat, S.B. Performance evaluation and techno-economic analysis of a novel building integrated PV/T roof collector: An experimental validation. *Energy Build.* **2014**, *76*, 164–175. [[CrossRef](#)]
11. Buker, M.S.; Riffat, S.B. Performance analysis of a combined Building Integrated PV/T Collector with a liquid desiccant enhanced dew point cooler. *Energy Proced.* **2016**, *91*, 717–727. [[CrossRef](#)]
12. Zondag, H.A.; Vries, D.W.; Helden, W.G.J.; Zolingen, R.J.C.; Steenhoven, A.A. The yield of different combined PV-thermal collector designs. *Sol. Energy* **2003**, *74*, 253–269. [[CrossRef](#)]
13. Tse, K.K.; Chow, T.T.; Su, Y. Performance evaluation and economic analysis of a full scale water-based photovoltaic/thermal (PV/T) system in an office building. *Energy Build.* **2016**, *122*, 42–52. [[CrossRef](#)]
14. Calise, F.; d'Accadia, M.D.; Vanoli, L. Design and dynamic simulation of a novel solar trigeneration system based on hybrid photovoltaic/thermal collectors (PVT). *Energy Convers. Manag.* **2012**, *60*, 214–225. [[CrossRef](#)]
15. Buonomano, A.; Calise, F.; Vicidomini, M. Design, simulation and experimental investigation of a solar system based on PV panels and PVT collectors. *Energies* **2016**, *9*, 497. [[CrossRef](#)]
16. Tiwari, A.; Sodha, M.S. Performance evaluation of solar PV/T system: An experimental validation. *Sol. Energy* **2006**, *80*, 751–759. [[CrossRef](#)]
17. Rodney, L.; Jones, D.E.; Cole-Appel, B.E. Calculation of performance of N collectors in series from test data on a single collector. *Sol. Energy* **1979**, *23*, 535–536.
18. Dubey, S.; Tiwari, G.N. Analysis of PV/T flat plate water collectors connected in series. *Sol. Energy* **2009**, *83*, 1485–1498. [[CrossRef](#)]
19. Shyam; Tiwari, G.N.; Al-Helal, I.M. Analytical expression of temperature dependent electrical efficiency of N-PVT water collectors connected in series. *Sol. Energy* **2015**, *114*, 61–76.
20. Dubey, S.; Tiwari, G.N. Analysis of different configurations of flat plate water collectors connected in series. *Int. J. Energy Res.* **2008**, *32*, 1362–1372. [[CrossRef](#)]
21. Shyam; Tiwari, G.N.; Fischer, O.; Mishra, R.K.; Al-Helal, I.M. Performance evaluation of N-photovoltaic thermal (PVT) water collectors partially covered by photovoltaic module connected in series: An experimental study. *Sol. Energy* **2016**, *134*, 302–313. [[CrossRef](#)]
22. Raju, V.R.; Narayana, R.L. Effect of flat plate collectors in series on performance of active solar still for Indian coastal climatic condition. *J. King Saud Univ. Eng. Sci.* **2016**. [[CrossRef](#)]
23. Mishra, R.K.; Tiwari, G.N. Energy and exergy analysis of hybrid photovoltaic thermal water collector for constant collection temperature mode. *Sol. Energy* **2013**, *90*, 58–67. [[CrossRef](#)]
24. Singh, S.; Agrawal, S. Efficiency maximization and performance evaluation of hybrid dual channel semitransparent photovoltaic thermal module using fuzzyfied genetic algorithm. *Energy Convers. Manag.* **2016**, *122*, 449–461. [[CrossRef](#)]
25. Zhang, J.; Li, X.; Zhao, T.; Dai, W. Experimental study on a novel fuzzy control method for static pressure reset based on the maximum damper position feedback. *Energy Build.* **2015**, *108*, 215–222. [[CrossRef](#)]
26. Lu, Z.; Zhang, J.; Chen, Y.; Zhan, T.; Liu, H. Fuzzy control model and simulation of supply air system in a test rig of low-temperature hot-water radiator system. *Energy Build.* **2010**, *42*, 386–392. [[CrossRef](#)]
27. Tillack, L.; Rishel, J.B. Proper control of HVAC variable speed pumps. *ASHRAE J.* **1998**, *11*, 42–47.
28. *Design Standard for Energy Efficiency of Public Buildings*; GB 50189-2005; China Building Industry Press: Beijing, China, 2005.
29. *Code for Design of Heating Ventilation and Air Conditioning*; GB 50019-2003; China Planning Press: Beijing, China, 2003.
30. Armstrong, P.R. Extension of the Hottel-Whillier-Bliss model to multi-stage collector systems. *Int. Telem. Conf. Proc.* **1978**, *2*, 173–176.

